Distributed vibration sensing of perimeter security based on space difference of Rayleigh backscattering

Shang Ying[1], Wang Chen[1], Wang Chang[1*], Liu Xiaohui[1], Sun Zhihui[1], Ni Jiasheng[1], Peng Gangding[1,2]

(1. Laser Institute, Qilu University of Technology(Shandong Academy of Sciences), Jinan 250014, China;

2. School of Electrical Engineering & Telecommunications, University of New South Wales, NSW 2052, Australia)

Abstract: A optical distributed vibration sensing(DVS) scheme based on the space difference of Rayleigh backscattering was presented for perimeter security. In this scheme Rayleigh backscattered light with phase changes induced by vibration signal along the sensing fiber was split and fed into an imbalanced Michelson interferometer. The space difference of Rayleigh backscattering was realized. The DVS system realized the phase demodulation of the Rayleigh backscattered light to improve the sensitivity of the system. The distributed vibration sensing system based on space difference of Rayleigh backscattering can restore the walking route, the velocity of the intruder and the distance of the simulative digger, and obtain the demodulated signal SNR of 15 dB and detection distance of 35 m.

Key words: distributed vibration sensing; perimeter security; interferometer; space difference

采用后向瑞利散射空间差分的周界安防分布式振动监测

尚　盈[1],王　晨[1],王　昌[1*],刘小会[1],孙志慧[1],倪家升[1],彭刚定[1,2]

(1. 齐鲁工业大学(山东省科学院),山东省科学院激光研究所,山东 济南 250014;

2. 新南威尔士大学 电气工程与电信学院,新南威尔士 2052)

摘　要: 提出了应用于周界安防的基于后向瑞利散射光空间差分干涉的光纤分布式振动传感监测方案。环境振动信号引起传感光纤的相位变化,含有相位信息的后向瑞利散射信号注入到非平衡迈克尔逊干涉仪,实现了后向瑞利散射信号的空间差分干涉,光纤分布式振动传感监测完成相位信号的解调,提高了系统的灵敏度。该系统能够实时监测入侵者的行走路线和速率以及模拟挖掘的距离的判断,实现了 15 dB 的信噪比以及 35 m 的探测距离。

关键词: 分布式振动传感; 周界安防; 干涉仪; 空间差分

0 Introdction

With the rapid development of society, remote monitoring and protection of some important areas has become increasingly important, such as airports, oil pipelines, frontier, nuclear power plants, prisons and so on. In the perimeter security system, the signal detection technology mainly includes active infrared detection technology[1], microwave detection technology[2], electro-magnetic field sensing technology[3] and optical fiber sensing technology[4].

Active infrared detection technology is the point-to-point detection, so it is just suitable for use in a small range of security systems. Microwave detection technology and electromagnetic field sensing technology is susceptible to weather or electromagnetic interference. The optical fiber has the the characteristics of passive detecion, anti-electromagnetic ability and so on. Especially, the fiber buried under the ground has the high degree of concealment. Therefore, the optical fiber distributed vibration detection technology is a very ideal technology for perimeter security detection. Up to now, optical fiber distributed measurement technology mainly consists of optical fiber interferometer technology and optical time/frequency domain reflection technology[5-7]. On the other hand, dual interferometers have been developed to get the position and information of the vibration along the sensing fiber, such as Sagnac-Sagnac[8-9], Sagnac-MZ[10-11], Sagnac-Michelson[12] and MZ-MZ[13-14]. However, the optical path design and demodulation algorithm of dual interferometers are complex, making it difficult to be implemented in practical application. Optical time domain reflection (OTDR) technology makes use of Rayleigh effects induced by external disturbance on the optical fiber[15]. Currently the conventional OTDR, phase-sensitive OTDR (φ-OTDR)[16-17] and the coherent OTDR (C-OTDR)[18] can be applied to the perimeter security detection. The conventional OTDR is the intensity demodulation based on broadwind source, so

the sensitivity of the system is limited. Φ-OTDR means coherent light source with direct detection. In this case, a kHz line-width laser is used with short pulses for coherent detection, because the Rayleigh backscattering in the fiber section covered by transmission of the short pulse is just interfered, the sensitivity cannot meet the requirement of the particular application. The C-OTDR make use of the local oscillator to intenfer with the Rayleigh backscattering, the polarization influences the system performance. However, we propose the optical DVS scheme based on the space difference of Rayleigh backscattering. In the scheme, the technique is based on measuring the phase between the Rayleigh backscattered light from two sections of the fiber which is according to the path difference of the imbalanced Michelson interferometer. The energy spectrum algorithm is applied to the perimeter security detection, and DVS system can record the route and velocity of the intruder, the distance of the simulative digger, and obtain the demodulated signal SNR of 15 dB and detection distance of 35 m.

1 Principle

We use the one-dimensional impulse-response model of the backscattering from a fiber to explain the system theoretically. When we launch a coherent light pulse with pulse-width W and optical frequency f into a fiber at t=0, we obtain a backscattered wave at the input end of the fiber which is given by[19]:

$$e_r(t) = \sum_{i=1}^{N} a_i \cos[2\pi f(t-\tau_i)] \mathrm{rect}\left(\frac{t-\tau_i}{W}\right) \qquad (1)$$

Where a_i and τ_i are the amplitude and delay of the ith Rayleigh backscattering respectively, N is the total number of Rayleigh backscattering, and rect$[(t-\tau_i)/W] = 1$, when $0 < (t-\tau_i)/W < 1$, and is zero otherwise. The delay τ_i corresponds to the distance z_i from the input end to the ith backscattering through the relation $\tau_i = 2n_f z_i/c$, n_f is the refractive index of the fiber. The term rect$[(t-\tau_i)/W]$ accounts for the change in the scattering volume seen as the pulse propagates.

As shown in Fig.1, the path difference of the imbalanced Michelson interferometer is s, so the delay signal $e_r(t)$ is written as:

$$e_{rs}(t) = \sum_{j=1}^{N} a_j \cos[2\pi f(t-\tau_i-\tau_s)] rect\left(\frac{t-\tau_j-\tau_s}{W}\right) \quad (2)$$
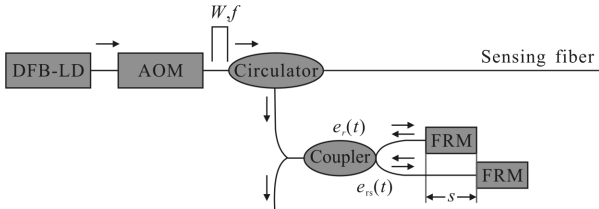

Fig.1 Achematic diagram of the interferometer of Rayleigh backscattering

Two reflected waves at the coupler interfere, the interferometer signal intensity $I(t)$ is given by

$$I(t) = [e_r(t)+e_{rs}(t)] \times [e_r(t)+e_{rs}(t)]^* = \sum_{i=1}^{N} \sum_{q=1}^{N} a_j a_q$$

$$\cos[2\pi f(\tau_i-\tau_p)] rect\left(\frac{t-\tau_i}{W}\right) + \sum_{i=1}^{N} \sum_{j=1}^{N} a_j a_p$$

$$\cos[2\pi f(\tau_j-\tau_q)] rect\left(\frac{t-\tau_j-\tau_s}{W}\right) + 2\sum_{i=1}^{N} \sum_{p=1}^{N} a_i a_j$$

$$\cos\left(\frac{4\pi f n_f}{c}\right) rect\left(\frac{t-\tau_i-\tau_s}{W}\right) rect\left(\frac{t-\tau_j-\tau_s}{W}\right) \quad (3)$$

As shown in Eq.(3), it is known that the interference signal contains phase information induced by the acoustic signal, so as long as phase information can be demodulated, the DVS system can quantitatively restore the vibration information.

2 Experiment

2.1 Experimental setup

The sensing cable is arranged into the trench whose size is 50 m×5 m for two circles, as shown in Fig.2, the bottom circle of sensing cable is 50 cm away from the ground, and the top circle of sensing cable is 25 cm away from the ground. The coil 1 of the fiber cable is used to connect the sensing cable to the DVS system. The coil 2 of the fiber cable is remained at the end of the sensing fiber.

The first experiment is the route detection of the intruder. The intruder walks along the direction of the

cable at the horizontal distance of 0, 0.5, 0.75, 1, 2 m away from the sensing cable.

The second experiment is the dropping detection. The solid ball strikes the ground in the free fall with the height of 1 m at different distance away from the sensing cable. At the distance of the 35 m away from the cable, the solid ball strikes the ground at different height of 0.5, 1, 1.5, 2 m.
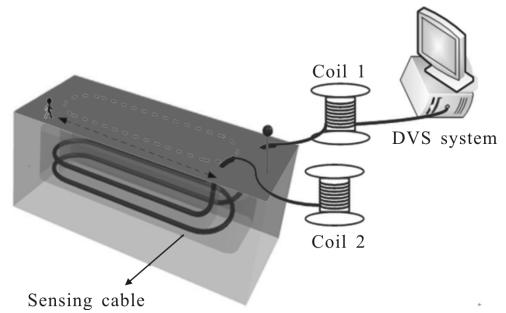

Fig.2 DVS experimental diagram

2.2 Experimental result and analysis

The DVS demodulated results of the intrusion are given from Fig.3 to Fig.5. Figure 3 shows the 2D demodulated result at the horizontal distance of 0 m away from the sensing cable. It can be clearly seen that there exist two curves because the cable of the top and bottom circle can pick up the intrusion signal. As shown in Fig.3, the DVS system has recorded the walking route that the intruder goes forth and back along the cable.
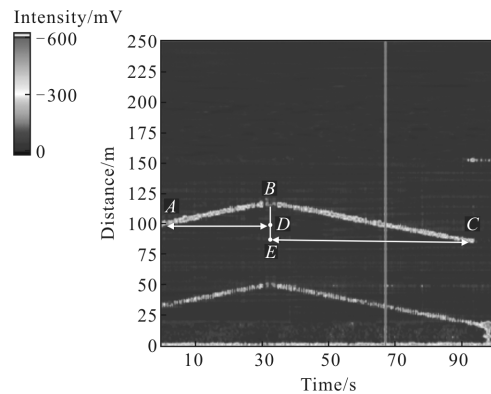

Fig.3 2D demodulated result of the DVS on the intrusion

If we figure out the distance of the BD (S_{BD}) and the time of AD (T_{AD}), the velocity of the intruder (V_{AB})

from position **A** to position **B** can be calculated accordding to the equation $V_{AB}=S_{BD}/T_{AD}$. The velocity of the intruder(V_{BC}) from position **B** to position **C** can alse be calculated in the same way. Figure 4 depicts the information of the time domain at the time of 68th second. There are the energy values obtained by the power spectrum of the demodulated phase at the postion of 30 m and 100 m in Fig.4 (a). Figure 4(b) depicts SNR of the DVS system which reaches 14 dB at the time of 68th second.
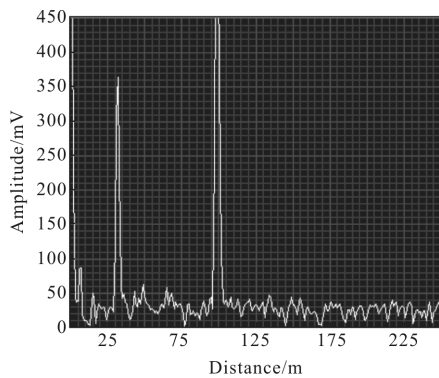
(a) Time domian information
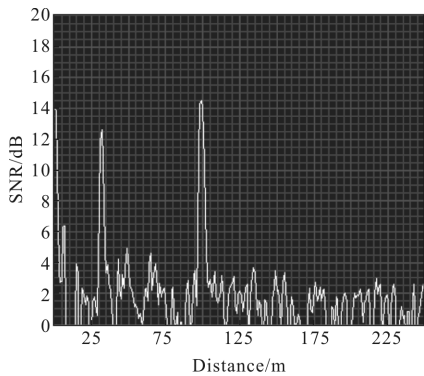
(b) SNR

Fig.4 Data analysis of the intrusion

Figure 5(a) shows the 3D demodulated result at the horizontal distance of 0 m away from the sensing cable. Two walking curves are more clearly seen in Fig.5(a). The experiment is done at different distance away from the cable. The data extracted at the position of 100 m is analyzed at the horizontal distance of 0, 0.5, 0.75, 1, 2 m away from the sensing cable in Fig.5(b).

As shown in Fig.5(b), the demodulated amplitude

value decreases as the horizontal distance increase. The DVS system can detect the intrusion signal of 2 m horizontal distance away from the cable.
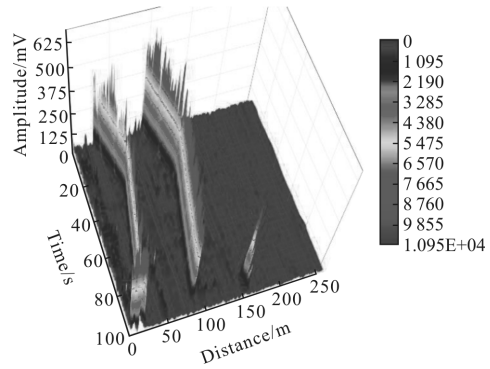
(a) Above the cable
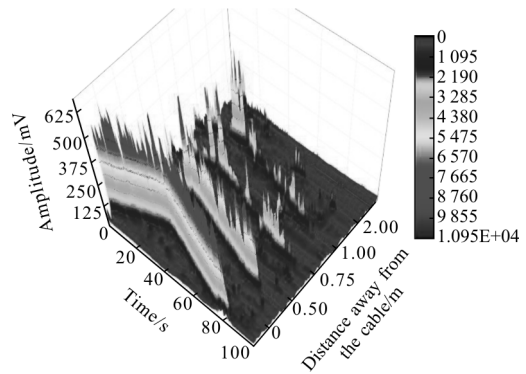
(b) Different distance away from the cable

Fig.5 3D demodulated result of the DVS on the intrusion with different distance

The DVS demodulated results of the dropping are shown from Fig.6 to Fig.9. The ball dropping is applied to simulate the digging. Figure 6 shows the 2D demodulated result at the horizontal distance of 0 m away from the sensing cable. As shown in Fig.6, there are clearly ten response curves according to the ten times of dropping. Figure 7 represents the information of the time domian at the time of 18th second. There are the energy values obtained by the power spectrum of the demodulated phase at the position of 80 m and 150 m in Fig.7(a). Figure 7(b) depicts SNR of the DVS system which reaches 15 dB at the time of 18th second.
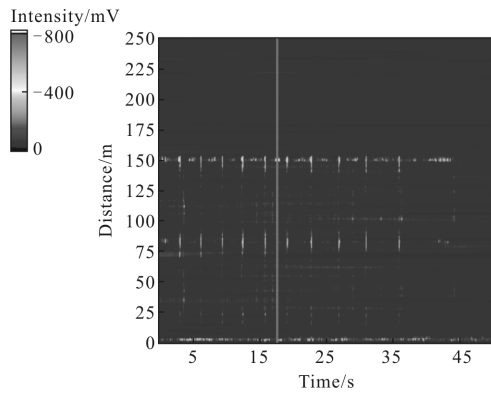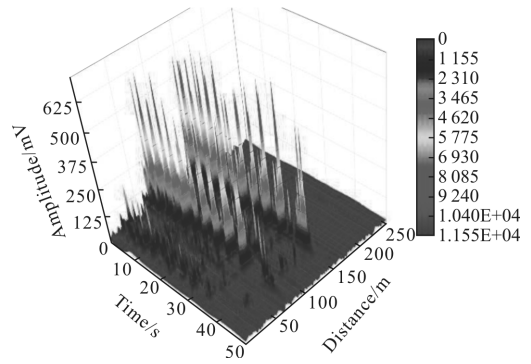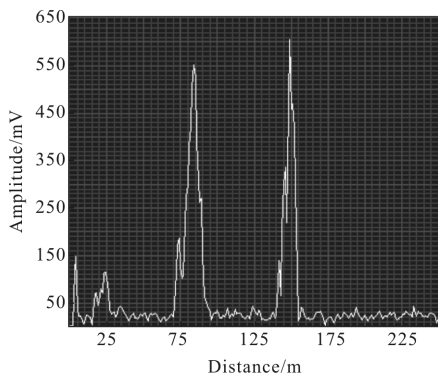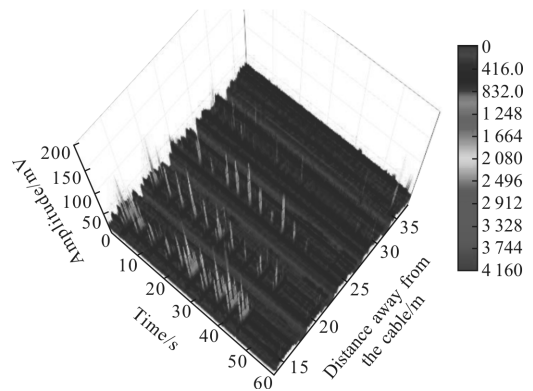
Fig.6 2D demodulated result of the DVS on the dropping

(a) Power spectrum

(b) SNR

Fig.7 Data analysis of the dropping

Figure 8 (a) shows the 3D demodulated result at different horizontal distance of 0 m away from the sensing cable. Ten response curves are more clearly seen in Fig.8(a). The experiment is done at different distance away from the cable. The data extracted at the position of 100 m is analyzed at the horizontal distance of 15, 20, 25, 30, 35 m away from the sensing cable in Fig.8(b).

(a) Above the cable
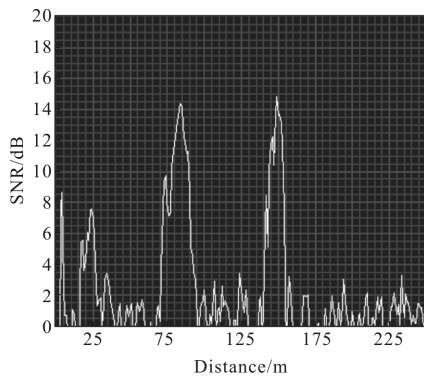

(b) Different distance away from the cable

Fig.8 3D demodulated result of the DVS on the dropping with different distance

Figure 9 depicts the 3D demodulated result at the 35 m horizontal distance away from the sensing cable
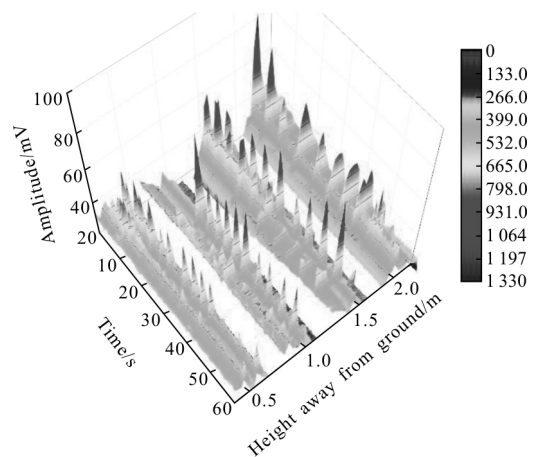

Fig.9 3D demodulated result of the DVS on the dropping with different height

with different height of 0.5, 1, 1.5, 2 m. As shown in Fig.9, there are still ten response curves to the

dropping. The demodulated amplitude value increases as the height increases. The DVS system can detect the dropping signal of 35 m horizontal distance away from the cable.

3 Conclusion

The optical DVS scheme based on the space difference of Rayleigh backscattering is proposed to perimeter security. In the scheme, the technique is based on measuring the phase between the Rayleigh backscattered light from two sections of the fiber which is according to the path difference of the imbalanced Michelson interferometer. The energy spectrum algorithm is applied to the perimeter security detection, and DVS system can record the route and velocity of the intruder, the distance of the simulative digger, and obtain the demodulated signal SNR of 15 dB and detection distance of 35 m.

References:

[1] Liu Kun, Chai Tianjiao, Liu Tiegen. Multi-area perimeter security system with quick invasion judgement algorithm [J]. Journal of Optoelectronics·Laser, 2015, 26 (2): 288–294. (in Chinese)

[2] Wang Mingji, Zhang Yong, Li Yushang. High precision perimeter intrusion detection alarm system based on single host [J]. Chinese Journal of Scientific Instrument, 2006, 27 (12): 1718–1720. (in Chinese)

[3] Gao Songwei, Yang Yang. Application of leakage coaxial cable in perimeter alarm device [J]. Journal of Shenyang University of Technology, 2006, 28(1): 91–93. (in Chinese)

[4] Alasaarela I, Karioja P, Kopola H K. Comparison of distributed fiber optic sensing methods for location and quantity information measurements [J]. Optical Engineering, 2002, 41(1): 181–189.

[5] Shang Ying, Wang Chen, Liu Xiaohui. Optical distributed acoustic sensing based on the phase optical time-domain reflectometry [J]. Infrared and Laser Engineering, 2017, 46 (3): 0321003.

[6] Lv Qiying, Li Lijing, Wang Hongbo. Influences of laser on fiber-optic distributed disturbance sensor based on $\varPhi$-OTDR [J]. Infrared and Laser Engineering, 2014, 43(12): 3918–

3923.

[7] Zhang Junnan, Lou Shuqin, Liang Sheng. Study of pattern recognition based on SVM algorithm for φ-OTDR distributed optical fiber disturbance sensing system [J]. Infrared and Laser Engineering, 2017, 47(4): 0422003. (in Chinese)

[8] He Cunfu, Feng Peipei, Ruan Li. Research on security early warning system based on dual-Sagnac interferometer [J]. Optical Technique, 2013, 39(6): 488–495. (in Chinese)

[9] Wu H. Dual-wavelength Sagnac interferometer as perimeter sensor with Rayleigh backscatter rejection [J]. Optical Engineering, 2014, 53(4): 044111.

[10] Chen Qingming, Jin Chao. A distributed fiber vibration sensor utilizing dispersion induced walk-off effect in a unidirectional Mach-Zehnder interferometer [J]. Optics Express, 2014, 22(3): 2167–2173.

[11] Wei Pu, Shan Xuekang, Sun Xiaohan. Frequency response of distributed fiber-optic vibration sensor based on nonbalanced Mach–Zehnder interferometer [J]. Optical Fiber Technology, 2013, 19(1): 47–51.

[12] Kondrat M, Szustakowski M, Palka N, et al. A Sagnac-Michelson fibre optic interferometer:signal processing for disturbance localization [J]. Opto-Electronics Review, 2007, 15(3): 127–132.

[13] Li J, Ning T, Pei L. Photonic generation of triangular waveform signals by using a dual-parallel Mach-Zehnder modulator [J]. Optics Letters, 2011, 36(19): 3828–3830.

[14] Jiang Lihui, Yang Ruoyu. Identification technique for the intrusion of airport enclosure based on double mach-zehnder interferometer [J]. Journal of Computers, 2012, 7(6): 1453–1458.

[15] Bao Xiaoyi, Chen Liang. Recent progress in distributed fiber optic sensors [J]. Sensors, 2012, 12: 8601–8639.

[16] Hui Xiaonan, Zheng Shilie, Zhou Jinhai. Electro-optic modulator feedback control in phase-sensitive optical time-domain reflectometer distributed sensor [J]. Applied Optics, 2013, 52(35): 8581–8585.

[17] Peng F, Wu H, Jia X H. Ultra-long high-sensitivity $\varPhi$-OTDR for high spatial resolution intrusion detection of pipelines [J]. Opt Express, 2014, 22(11): 13804–13810.

[18] Lu Yuelan, Zhu Tao. Distributed vibration sensor based on coherent detection of phase –OTDR [J]. Journal of Lightwave Technology, 2010, 28(22): 3243–3248.

[19] Juskaitis R, Mamedov A M, Potapov V T. Interferometry with Rayleigh backscattering in a single-mode optical fiber [J]. Optics Letters, 1994, 19(3): 225–227.